Biochimica et Biophysica Acta 1853 (2015) 1850–1859

Contents lists available at ScienceDirect

Biochimica et Biophysica Acta

journal homepage: www.elsevier.com/locate/bbamcr

A presequence-binding groove in Tom70 supports import of Mdl1 into mitochondria

Jonathan Melin [a], Markus Kilisch [b], Piotr Neumann [c], Oleksandr Lytovchenko [a], Ridhima Gomkale [a], Alexander Schendzielorz [a], Bernhard Schmidt [a], Thomas Liepold [d], Ralf Ficner [c], Olaf Jahn [d], Peter Rehling [a,e,*], Christian Schulz [a]

[a] Institute of Cellular Biochemistry, University Medical Center Göttingen, Germany
[b] Department of Molecular Biology, University Medical Center Göttingen, Germany
[c] Department of Molecular Structural Biology, University of Göttingen, Germany
[d] Proteomics Group, Max Planck Institute of Experimental Medicine, Göttingen, Germany
[e] Max Planck Institute for Biophysical Chemistry, Göttingen, Germany

ARTICLE INFO

Article history:
Received 2 March 2015
Received in revised form 23 April 2015
Accepted 30 April 2015
Available online 7 May 2015

Keywords:
Tom70
Mitochondria
Protein import
Presequence

ABSTRACT

The translocase of the outer mitochondrial membrane (TOM complex) is the general entry gate into mitochondria for almost all imported proteins. A variety of specific receptors allow the TOM complex to recognize targeting signals of various precursor proteins that are transported along different import pathways. Aside from the well-characterized presequence receptors Tom20 and Tom22 a third TOM receptor, Tom70, binds proteins of the carrier family containing multiple transmembrane segments. Here we demonstrate that Tom70 directly binds to presequence peptides using a dedicated groove. A single point mutation in the cavity of this pocket (M551R) reduces the presequence binding affinity of Tom70 ten-fold and selectively impairs import of the presequence-containing precursor Mdl1 but not the ADP/ATP carrier (AAC). Hence Tom70 contributes to the presequence import pathway by recognition of the targeting signal of the Mdl1 precursor.

1. Introduction

Survival of eukaryotic cells depends on the presence of functional intracellular organelles. Amongst them, mitochondria are crucial to provide energy and essential iron–sulfur clusters. To fulfill these functions, mitochondria import nuclear-encoded proteins in a post-translational manner [1–4]. Additionally, co-translational import might be relevant for a set of precursor proteins [5,6]. Transport of the precursor proteins to their various sub-mitochondrial compartments involves several different import pathways [1,3]. In recent years, it became clear that a regulation of these import pathways is important for the integration of cellular signals, such as the adaptation to nutrients and progression through the cell cycle [4,7].

A major target of regulation is the translocase of the outer mitochondrial membrane (TOM complex), the general entry gate for almost all imported proteins. The import pathways of the different substrate classes converge at the TOM complex, which contains several receptor subunits. Tom20 and Tom22 recognize the N-terminal targeting signal (presequence) of precursor proteins destined for the mitochondrial matrix. The subsequent transport of these precursors through the TOM complex is then mediated by the small Tom5 and the channel-forming Tom40 [8–11]. The presequence is characterized by its ability to form an amphipathic α-helix. The net positive charge of the presequence is essential for the membrane potential driven transport of the precursor across the inner membrane, a process that is mediated by the presequence translocase of the inner membrane (TIM23 complex) [4]. In addition to the presequence, directing the precursor to the mitochondrial matrix, these substrates can also contain transmembrane segments that lead to their insertion into the inner mitochondrial membrane. This occurs by lateral release from the TIM23 complex but may also involve export of transmembrane segments from the matrix into the inner membrane by the OXA1 insertase [12,13].

One precursor that is transported along this import route is the ABC transporter Mdl1. After import of its N-terminus and lateral release of the first two transmembrane segments, the following two transmembrane domains are initially imported into the matrix. Subsequently, OXA1 inserts them into the inner membrane from the matrix side while transmembrane segments five and six are again laterally released from the TIM23 complex [13]. After assembling into a homodimer, Mdl1 facilitates the ATP-dependent export of peptides (6–20 amino acids) from the mitochondrial matrix into the intermembrane space [14]. As Mdl1 does not transport random peptides, it is thought to have specific

* Corresponding author at: Institute of Cellular Biochemistry, University Medical Center Göttingen, Humboldtallee 23, 37073 Göttingen, Germany. Tel.: +49 551 39 5947.
E-mail address: Peter.Rehling@medizin.uni-goettingen.de (P. Rehling).

http://dx.doi.org/10.1016/j.bbamcr.2015.04.021
0167-4889/

substrates yet to be elucidated [15]. Other substrates, which are sorted into the inner membrane by the combined action of TIM23 and OXA1 include Mdl2 and Shd4 [16,17].

A third receptor of the TOM complex, Tom70, recognizes proteins of the carrier family, which contain multiple transmembrane segments and utilize internal targeting signals. Tom70 recognizes these signals in the precursor as well as the substrate-associated Hsp70 chaperones and subsequently releases the chaperones in an ATP dependent manner [18–20]. Upon translocation across the TOM complex and arrival in the intermembrane space, the hydrophobic carrier substrates engage with the hexameric complexes of the small Tim proteins. These guide the precursor to the carrier translocase (TIM22 complex), which facilitates membrane potential-dependent insertion into the inner mitochondrial membrane [1,21]. Substrates of the carrier pathway include not only the ADP/ATP carrier (AAC) and the phosphate carrier, but also subunits of inner membrane protein translocases (Tim23, Tim17, Tim22).

In addition to the contribution to carrier protein import, Tom70 has also been implicated in the import of presequence-containing proteins [22–25], though this contribution of Tom70 has been controversial [26–28]. In the last years, significant structural insight into Tom70 revealed that the tetratricopeptide repeats (TPR) 1–3 in the N-terminal part of the protein bind to the C-terminal EEVD motif of Hsp70 and Hsp90 [20,29]. By contrast, a pocket in the C-terminal domain containing TPR4-11, was proposed to function as the potential binding cleft for the hydrophobic carrier substrates [20,29,30].

In the present study we utilized presequence photo-peptides to characterize presequence-binding sites in the TOM complex. We identified Tom70 as a presequence receptor and mapped the binding site to the previously proposed carrier substrate-binding pocket. Identification of a point mutant in this binding groove functionally demonstrated the recognition of presequence peptides by this binding site. The specific impairment of presequence-containing Mdl1 import, but not of carrier substrates, indicates that Tom70 contributes to presequence import by specific recognition of the targeting signal within a subset of presequence substrates.

2. Materials and methods

2.1. Yeast strains and growth conditions

Saccharomyces cerevisiae YPH499 was used as the wild-type strain and was cultured in YPG medium (1% yeast extract, 2% peptone, 3% glycerol) at 30 °C. In the background of the genomic deletion of *TOM70* described earlier [31], *TOM71* was deleted using a kanamycin marker. The resulting *Tom70*Δ/ *tom71*Δ was transformed with pRS416 containing no insert (*tom70*Δ/ *tom71*Δ) or wild-type *TOM70* (promotor, ORF and terminator). The M551R mutant was generated using site-directed mutagenesis of the wild-type *TOM70* plasmid and also transformed into the genomic *TOM70* deletion strain. The *tom70*Δ/ *tom71*Δ, wild-type (*TOM70*) and *TOM70*^{M551R} cells were grown on selective medium lacking uracil (0.67% yeast nitrogen base, 3% glycerol, 0.07% complete supplement mixture without uracil). Mitochondria were isolated as described before [32].

2.2. Photo cross-linking and mass spectrometric analysis of photo-adducts

In organello photo cross-linking with $pL_{19}B$ and $pS_{16}B$ was carried out as described earlier [33]. Essentially, mitochondria were suspended in import buffer lacking BSA (250 mM sucrose, 10 mM MOPS/KOH, 80 mM KCl, 2 mM KH_2PO_4, 5 mM $MgCl_2$, 5 mM Methionine, pH 7.2) at 1 μg/μl and incubated with 2 μM of photo-peptide for 10 min on ice prior to UV irradiation for 30 min on ice. A halogen vapor lamp was combined with a filter to avoid protein-damaging wavelengths below 300 nm [34]. Samples were analyzed by SDS–PAGE and Western blotting.

For purification of photo-adducts 1.6 μg/μl mitochondria were photo cross-linked with 2 μM photo-peptides as described above. Subsequently, mitochondria were washed with SEM buffer (250 mM sucrose, 20 mM MOPS/KOH, 1 mM EDTA, pH 7.2) and resuspended in lysis buffer (50 mM Tris/HCl pH 7.4, 1% SDS, 1 mM EDTA, 6 M urea) at 10 μg/μl. After incubation for 10 min at 25 °C the solubilizate was diluted to 1 μg/μl with lysis buffer lacking urea and SDS but containing 0.1% Triton X-100, 2 μg/ml leupeptin and 2 mM 4-(2-aminoethyl)benzenesulfonyl fluoride hydrochloride. Following centrifugation the supernatant was loaded on streptavidin–agarose (Thermo Scientific) and bound proteins were eluted by incubation with protein loading buffer (2% SDS, 10% glycerol, 60 mM Tris/HCl, pH 6.8, 0.01% bromphenole blue, and 1% 2-mercaptoethanol) at 95 °C for 15 min.

Wild-type Tom70^{cd} (residues 43–622) was expressed in *Escherichia coli* BL21 from pET-19b with a N-terminal 10x His-tag essentially as described before [28]. M551R Tom70^{cd} was generated by site-directed mutagenesis and purified in the same way.

In vitro photo cross-linking was carried out using 4.5 μg purified wild-type protein and 5 μM $pL_{19}B$ with the same cross-linking procedure described above.

Identification of cross-linked residues was performed after in-gel digestion using trypsin, reverse phase chromatography and mass spectrometric analysis (LC MALDI MS/MS) as described previously [33]. Fragment ion mass spectra were converted into merged data files of the mgf format, which were analyzed with StavroX 3.4.11, a software tool for identifying cross-linked peptides with mass spectrometry [35]. Mass precision of precursor and fragment ions were set to 20 ppm and 0.7 Da, respectively, and only a-, b-, and y-type ions with a signal to noise ratio above 1.5 were considered for comparison with theoretical fragment ion masses. Three missed tryptic cleavages were allowed. Selection of candidate cross-link spectra for further manual validation was based on score and distribution of false-positive hits from a decoy dataset.

2.3. Modeling of Tom70-presequence interaction

The structure of the $pL_{19}B$ photo-peptide was modeled using the Abalone (http://www.biomolecular-modeling.com/Abalone/index.html) program assuming α-helical conformation. The C-terminal amino acids used as affinity tags were not modeled and the BPA residue has been modeled as a Tryptophan residue. Open and semi-open conformations of Tom70 (PDB ID: 2GW1) have been modeled based on superposition with Tom71 structure in the open state (PDB ID: 3LCA) [20,30]. Prior to docking calculations, conformations of protein side chains were optimized and remodeled using prepack protocol as implemented in the Rosetta FlexPepDock application [36]. Blind docking calculations have been set up using MGLTools software [37]. Initial blind docking was performed against Tom70 in both open and semi-open states using AutoDock Vina [38], keeping rotatable bonds of larger side chains (Arg, Leu, Trp, Met, Trp) flexible during docking. Several runs of AutoDock Vina were performed with altered exhaustiveness parameter values (16, 32 and 64). The distance limits for the spatial restraints provided by the cross-links have been estimated conservatively, assuming that amino acid side chains are fully extended and cross-links take place at the atom most distal to the Cα atom. For methionine and isoleucine side chains, the maximal distance spanned was estimated as 4.7 Å and 4.5 Å, respectively. These values were added to the maximal distance spanned by BPA (9.6 Å), resulting in 14.3 Å for Met-BPA and 14.1 Å for Ile-BPA cross-links [39].

The docking results were initially filtered based on Cα–Cα distances calculated between the BPA residue (modeled as Trp) and Met216, Met551 and Ile604 using a range of 5.0 to 16.0 Å. Analysis of docking calculations revealed that decoys fulfilling constraints from cross-linking experiments were obtained for the semi-open conformation of Tom70. However, several docking models of $pL_{19}B$ to Tom70 in the open conformation were similar to those obtained for semi-open

state, but with distances to Met216 exceeding the 15 Å limit. Those models have been included in the cluster analysis. Decoys corresponding to cluster center served as a starting orientation for high resolution docking using the FlexPepDock protocol as implemented in Rosetta software [36] using the semi-open conformation of Tom70. For each starting orientation, 1000 decoys have been generated and energetically scored and filtered by the constraints obtained from chemical cross-linking. The best decoys were then selected based on Rosetta score.

2.4. SPR analysis

SPR studies were carried out on a Reichert SR 7500 DC biosensor with NiHC1000m sensor chips obtained from Xantec Bioanalytics (Duesseldorf, Germany) [40]. Binding assays were performed in running buffer containing 50 mM HEPES pH 7.4, 150 mM NaCl and 50 μM EDTA, at a flow rate of 40 μl/min. Ligands (Tom70 variants) were immobilized onto the left channel of a Ni^{2+}-activated sensor chips at a flow rate of 30 μl/min, to a surface density of 3500–4000 μ RIU. The right channel served as a reference channel. Increasing concentrations of synthetic presequence peptide pCox4 and the control peptide SynB2 [33] were injected to both channels and the difference between the left and right channel was recorded. All analyte injections were further referenced by subtracting the average response of two buffer (blank) injections. Equilibrium binding and kinetic analysis were performed using Scrubber 2.0 (BioLogic Software).

2.5. Miscellaneous

Precursor proteins were radiolabeled and imported according to published procedures [33,41]. Quantifications of autoradiograms were carried out using ImageQuant TL (GE Healthcare). BN–PAGE, SDS–PAGE and Western blotting were performed according to standard procedures. Proteins were detected using fluorescent dye coupled secondary antibodies (LI-COR) using a FLA-9000 scanner (GE Healthcare) or by enhanced chemiluminescence. Colloidal coomassie staining was performed according to [42].

3. Results and discussion

3.1. Identification of a direct interaction between presequences and Tom70

Tom5, Tom20, Tom22 and Tom40 represent known presequence receptors of the TOM complex [4]. By contrast, the contribution of Tom70 to presequence import has remained controversial. In this study we set out to identify and characterize new presequence binding sites in the TOM complex using photoaffinity-labeling. To this end we utilized presequence photo-peptides based on the aldehyde dehydrogenase (pALDH) from rat, modified with a biotin and a His tag at the C-terminus, and a benzoyl-phenylalanine (BPA) on either the hydrophobic ($pL_{19}B$) or hydrophilic ($pS_{16}B$) side of the amphipathic helix (Fig. 1A) [33]. We could previously show that these modifications neither altered the targeting capacity of the presequence peptides nor impaired the mitochondrial integrity [33]. UV-activation of the BPA moiety in proximity to a target protein generates covalent linkages (primarily carbon–carbon bonds), which are sufficiently stable to be subsequently analyzed by mass spectrometry and hence allow mapping of the cross-linked residues.

In organello photo cross-linking of these photo-peptides with isolated wild-type mitochondria and subsequent Western blot analysis revealed photo-adducts with known presequence binding partners, such as Tim50 and Tom40, while proteins that do not display presequence recognition physiologically did not form covalent adducts with the photo-peptides (Fig. 1B) [11,33]. Interestingly, we observed photo-adducts between presequence peptides and Tom70, which were not as evident as in the case of smaller proteins due to the smaller relative size shift. To demonstrate that the widened Tom70 band obtained in lanes 2 and 3 (Fig. 1B) contained photo-peptide adducts, we isolated the photo-adducts using streptavidin–agarose following *in organello* photo cross-linking (Fig. 1C). The established and characterized photo-adducts of Tom40 and Tim50 were specifically isolated. In addition, Tom70 photo-adducts were recovered by this affinity purification.

Collectively, these results show that Tom70, the receptor of carrier proteins with internal targeting signals, can be cross-linked to presequence photo-peptides *in organello*, indicating a specific recognition event.

3.2. Identification of the presequence binding site in Tom70

Since the cross-linking radius of BPA is relatively large, these experiments cannot exclude that the presequence is bound by another receptor and cross-linked to Tom70 due to a favorable orientation of the cross-linker. In order to establish whether the photo-adduct formation observed *in organello* occurred due to direct presequence binding by Tom70, we purified the cytosolic domain of Tom70 from *E. coli* (Fig. 2A lane 1). *In vitro* cross-linking of this domain with $pL_{19}B$ allowed efficient generation of preparative amounts of the covalent photo-adducts (Fig. 2A lane 2). As both peptides showed a similar cross-linking efficiency, we restricted our analysis to the interaction with $pL_{19}B$. Following trypsin digestion, LC MALDI MS/MS analysis, and data analysis with StavroX, we identified several candidate cross-linked peptides (Table 1). In-depth manual validation of the mass spectra revealed significant adducts of $pL_{19}B$ to Met216, Met551, Ile604 and Met617, and the annotated fragment ion mass spectrum for Met551 is shown as an example in Fig. 2B.

Wu and Sha previously reported the crystal structure of Tom70 (resolved amino acids 94–607) [20]. Structural analysis revealed that the cross-linked residues are exclusively located on the buried surface forming a groove (Fig. 2C and D). While the crystal structure of Tom70 represents the closed conformation of the receptor, structures of its paralog, Tom71, revealed that the N- and C-terminal domains can change their relative position, exposing the groove to the solvent [20,29,30,43,44]. Taking this flexibility into account, we modeled Tom70 in the open state, performed blind docking of the presequence peptide to this model and selected those decoys which fulfilled our cross-linking constraints (see Materials and methods). This analysis revealed that a presequence peptide would fit into the groove present in Tom70 in the open conformation (Fig. 2D). However, as Met216 is located at the outer rim of the groove and the distance between the BPA and Met216 is larger than 15 Å under these conditions, we additionally modeled a semi-open state of Tom70 with Met216 located on the grooves wall. In this state the N- and C-terminal domains are moved slightly towards each other as compared to the open state (Fig. 2E). This conformation satisfies all cross-linking constraints at the same time.

Taken together, the analysis of the cross-linking sites revealed that presequences bind to a groove in Tom70. Binding of presequence peptides to Tom70 is direct and independent of other Tom subunits. Furthermore, due to the short length of the peptides used here, we can exclude the possibility that the mature portion of the protein mediates this binding. While the initial report on the structure of Tom70 highlighted the hydrophobic nature of the groove, subsequent structural studies revealed that the positional flexibility of the N- and C-terminal domains relative to each other disrupts this hydrophobic patch and exposes several polar residues [29,30]. It seems that this modulation of the binding cleft is required for the recognition of presequences as only the semi-open and open conformation of Tom70 could accommodate the presequence peptide and fulfill the cross-linking constraints. These conformations would allow presequence binding while at the same time the N-terminal domain would be available for the interaction with Hsp70 (R171 in Fig. 2C–E). These results are in line with earlier speculations that binding of Hsp70/Hsp90 could prevent

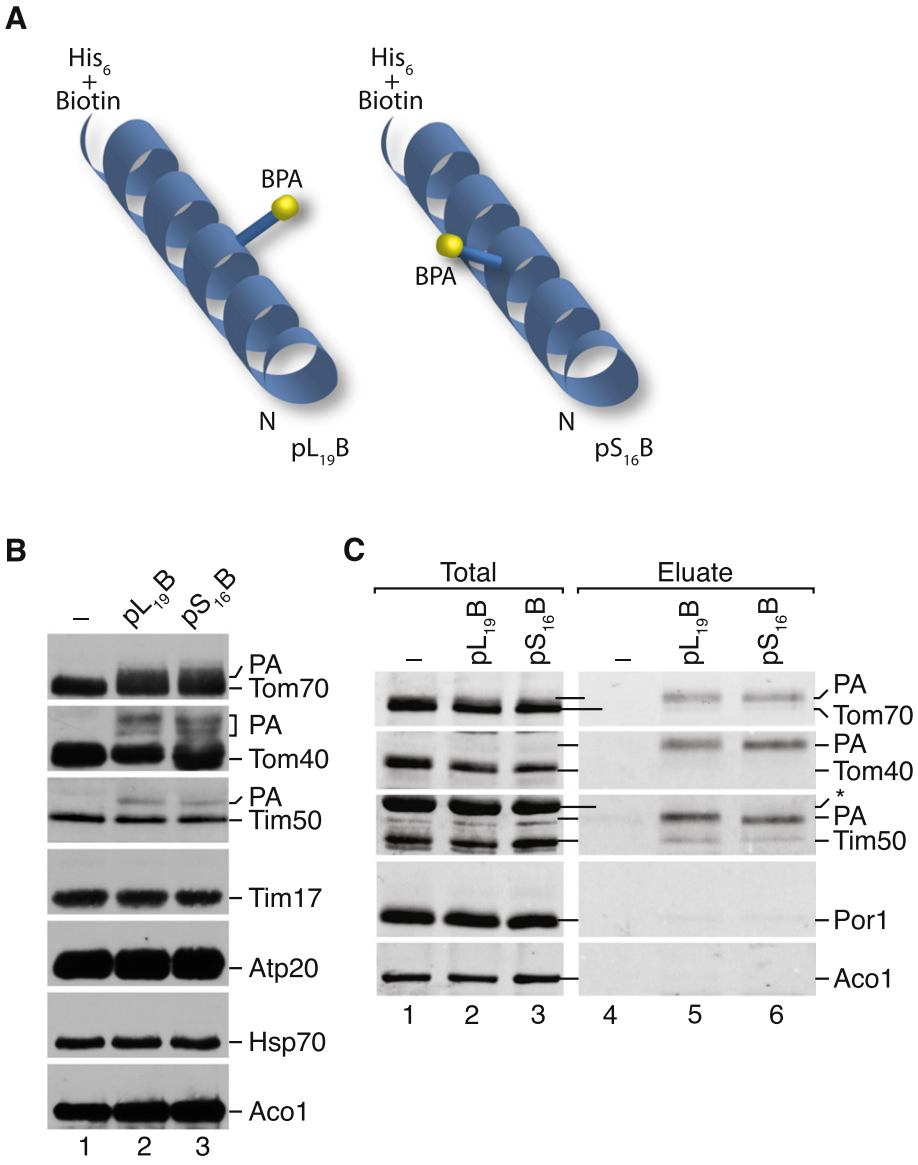

Fig. 1. Identification of a Tom70-presequence interaction. *A)* Illustration of the utilized synthetic photo-peptides. They are based on the rat alhdehyde dehydrogenase presequence containing a C-terminal biotinyl–Lysine (Biotin) and a 6x Histidine tag as well as p-benzoyl-Phenylalanine (BPA, yellow ball) at position 19 or 16 for $pL_{19}B$ or $pS_{16}B$, respectively. The Leu19 and Ser16 locate to the hydrophobic and hydrophilic side of the amphipathic helix, respectively. *B) In organello* UV photo cross-linking using buffer, $pL_{19}B$ or $pS_{16}B$. Samples were analyzed by SDS–PAGE and Western blotting. PA, photo-adducts. *C)* Photo cross-linking as in B, subsequently photo-adducts (PA) were affinity-isolated using streptavidin agarose. Eluates were analyzed as in B. Asteriks — unspecific signal.

Tom70/Tom71 from returning to the closed conformation and hence allow substrate binding [29,30].

3.3. Quantitative analysis of presequence binding to Tom70

While the cross-linking analysis allowed us to demonstrate the direct binding of presequence peptides to a presequence binding site in Tom70, this methodology does not allow for a quantitative assessment of the interaction. Therefore, we used purified wild-type cytosolic domain of Tom70 to determine its affinity to the presequence of the cytochrome *c* oxidase subunit 4 (pCox4) using surface plasmon resonance (SPR). Binding of pCox4 to $Tom70^{cd}$ reflected a bimolecular interaction with an affinity of 2.3 μM (Fig. 3A). Similar affinities have previously been determined for the presequence/Tim50 interaction [40]. Interestingly, the affinity of Tom20 to pALDH was reported to be ten-fold lower, however using a different methodology [9]. The control peptide SynB2 did not bind to $Tom70^{cd}$, supporting the notion that the presequence recognition is a specific binding event (Fig. 3B and C).

In order to confirm the physiological relevance of presequence binding by Tom70, we screened a wide variety of different mutations in the binding cleft. Amongst them, the Met551 to Arg exchange resulted in a soluble protein that could be efficiently purified from *E. coli*. Met551 was identified as the most prominent cross-linked residues in our mass spectrometric analysis (Fig. 2C) and is in close proximity to the presequence helix in the interaction model (Fig. 2D). SPR analysis with the pCox4 peptide showed a reduced presequence binding affinity of this mutant (Fig. 3D). As expected, the control peptide SynB2 showed no interaction with $Tom70^{M551R}$ (Fig. 3E and F).

In summary, Tom70 binds directly to pCox4 peptides *in vitro* with an affinity of 2.3 μM and the M551R mutation reduces Tom70's presequence affinity ten-fold (Fig. 3G).

3.4. Mutation of Met551 in Tom70 selectively affects Mdl1 import

In order to investigate the functional impact of the decreased presequence binding to $Tom70^{M551R}$ on protein import, we generated

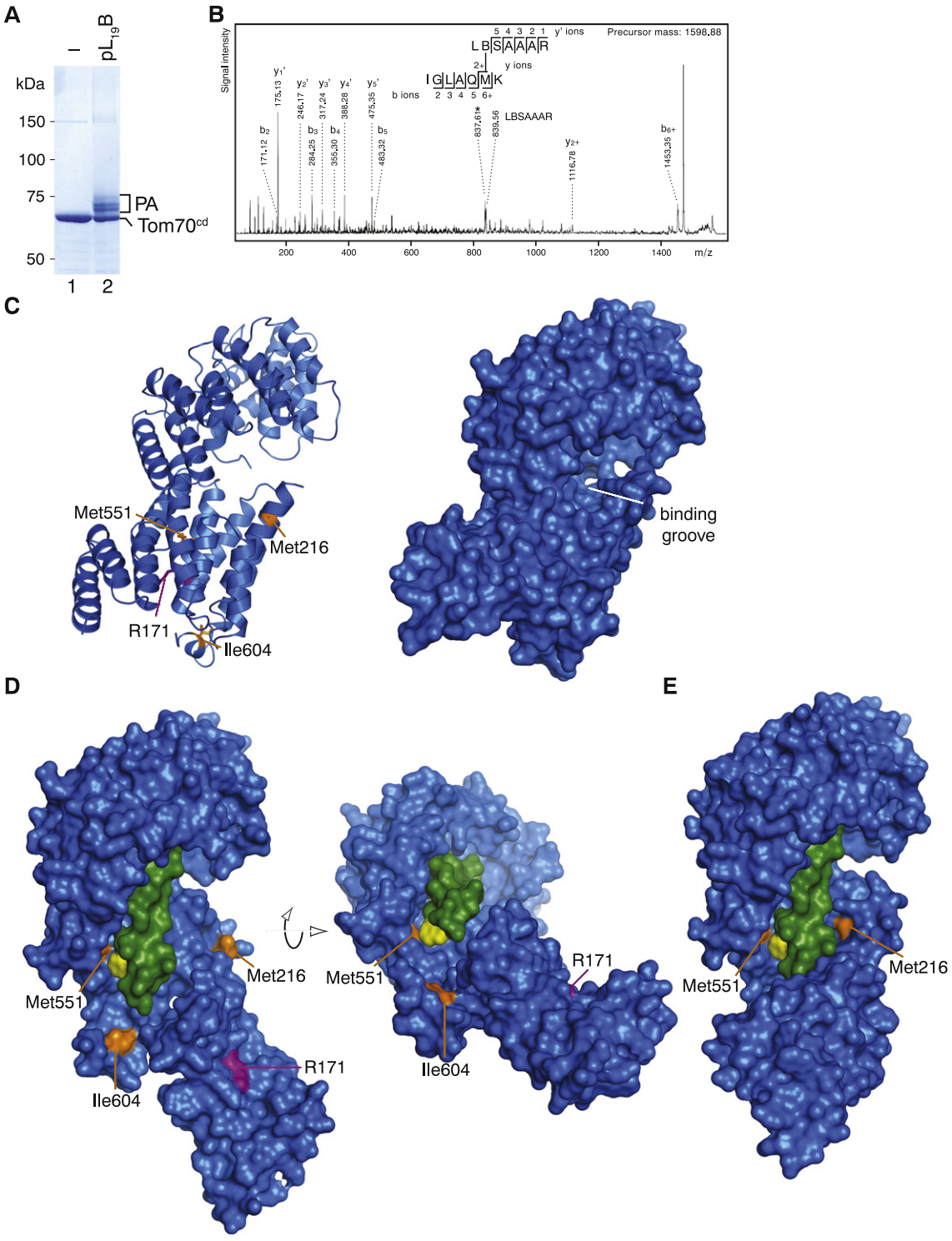

Fig. 2. Mapping the presequence binding site in Tom70. *A)* Purified Tom70 cytosolic domain (Tom70^{cd}) was *in vitro* photo cross-linked using only buffer (−) or pL$_{19}$B. Samples were analyzed by SDS–PAGE and colloidal coomassie staining. PA, photo-adducts. *B)* Photo-adducts generated in A were digested with trypsin and the peptides subjected to LC MALDI MS/MS analysis. Fragment ion mass spectrum of Tom70$^{546–552}$ cross-linked to pL$_{19}$B$^{18–24}$ ([M + H]$^{+}_{meas}$, 1598.88; [M + H]$^{+}_{calc}$, 1598.88), indicating Met551 of Tom70 as the cross-linking site. Only the b-, and y-ions (marked with + when carrying a cross-link to tryptic fragments of pL$_{19}$B) are indicated for the sake of clarity. Fragment ions resulting from cleavage of the cross-link bond are labeled with the respective tryptic peptide sequence. Asterisks indicate characteristic signals that are frequently observed after fragmentation of cross-linked methionine side chains [11,33,56]. *C)* Structural model of yeast Tom70 (PDB ID: 2GW1; residues 94–607) as cartoon (left). Amino acids found to be photo cross-linked to the presequence peptides are colored in orange (Met216, Met551, Ile604). Met617 is not shown. Arg171 (purple) indicates the Hsp70 binding site. The surface representation (right) shows the binding groove in its closed state. *D)* Surface representation of a possible binding mode of pL$_{19}$B (green) to Tom70. The open, binding competent, state of Tom70 was generated by homology modeling using the open Tom71 structure (3LCA). In this conformation, the N-terminal domain folds away from the C-terminal segment. The α-helical presequence peptide was docked using AutoDock Vina and resulting structures were selected based on the distance constraints obtained from the photo cross-linking analysis (Met-BPA 14.3 Å; Ile-BPA 16.1 Å). Following cluster analysis a few selected initial docking models were refined using FlexPepDock and the obtained decoys were energetically scored. The best model is presented. Left side shows a similar orientation as in C, on the right side the molecule is turned backwards to look down the presequence helix. Residue 19 in pL$_{19}$B is colored in yellow. *E)* Surface representation of the binding of pL$_{19}$B to the semi-open state of Tom70, which was generated by homology modeling using the open Tom71 structure. The binding mode of the presequence peptide is the same as in D, only that the N-terminal domain of Tom70 was moved towards the C-terminal domain. In this state all cross-link constraints, including the distance to Met216, are satisfied.

Table 1
StavroX analysis of the photo-adducts generated between $Tom70^{cd}$ and $pL_{19}B$ in Fig. 2A. After digestion with trypsin, the peptides were subjected to LC MALDI MS/MS analysis and the fragment ion mass spectra were analyzed as described in the Materials and methods Section. Only candidate cross-link spectra with a StavroX score larger than 25 were considered for manual validation. In the validation process, candidates represented by spectra that did not clearly point to a single cross-linked residue or contained numerous unassignable signals of considerable abundance were excluded from further study (colored in gray). The measured and calculated masses, deviations, the tryptic fragments of Tom70 and the identified cross-linked residues are shown. B represents carbamidomethyl–cystein.

Score	m/z	z	Mass (meas.)	Mass (calc.)	Dev (ppm)	Tom70 peptide	From	To	Site in Tom70
264	1598.878	1	1598.878	1598.872	3.67	[IGLAQMK]	546	552	Met551
108	1769.003	1	1769.003	1768.996	3.94	[KIQETLAK]	603	610	Ile604
94	1415.700	1	1415.700	1415.699	1.01	[EQGLM]	613	617	Met617
47	2565.253	1	2565.253	2565.255	−1.08	[GQMNFILQNYDQAGK]	404	418	
30	1631.837	1	1631.837	1631.846	−5.51	[VVEMSTK]	151	157	
29	1402.715	1	1402.715	1402.715	0.07	[QAMSK]	214	218	Met216
25	3457.646	1	3457.646	3457.710	−18.41	[EDPVFYSNLSABYVSVGDLK]	130	149	
22	1476.739	1	1476.739	1476.712	18.12	[NDFDK]	479	483	
22	1126.619	1	1126.619	1126.637	−16.18	[IR]	594	595	
22	1126.619	1	1126.619	1126.637	−16.18	[LR]	611	612	
18	1767.993	1	1767.993	1768.012	−10.49	[ALELK]	125/158	129/162	
17	3070.478	1	3070.478	3070.473	1.65	[GQMNFILQNYDQAGKDFDK]	404	422	

a *tom70*Δ/*tom71*Δ strain containing an empty plasmid or plasmids encoding wild-type or mutant Tom70. While the function of Tom71 remains unclear, we wanted to exclude a possible compensation by Tom71 due to its high sequence identity (53%) and similarity (70%) to Tom70 [45]. Isolation of mitochondria from these strains and analysis of the steady state protein levels revealed that the M551R mutation did not affect the stability of Tom70 (Fig. 4A). Furthermore the levels of other TOM components or control proteins were not affected by the mutation.

The main function of Tom70 is the recognition of carrier substrates and the release of chaperones bound to them, before their transfer to the Tom40 channel. In the absence of *tom70*Δ/ *tom71*Δ the import and assembly of carrier substrates, such as AAC, is significantly reduced (Fig. 4B) [46–49]. By contrast, the import of typical presequence-containing substrates does not depend on Tom70/ Tom71. In fact import of Su9-DHFR (a fusion protein consisting of the presequence of *Neurospora crassa* subunit 9 of the ATP synthase and mouse dihydrofolate reductase) is stimulated in the *tom70*Δ/ *tom71*Δ (Fig. 4C). This inverse correlation between the import of TIM23 (presequence) and TIM22 (carrier) substrates has been observed before but the explanation remains elusive [33,50–53]. By contrast to the *tom70*Δ/ *tom71*Δ, $tom70^{M551R}$ supported import and assembly of AAC with the same efficiency as the wild-type (Fig. 4D). This is in line with the unaltered steady state levels of Tim23, a TIM22 substrate (Fig. 4A). Furthermore, matrix import of the model presequence substrate Su9-DHFR into $tom70^{M551R}$ mitochondria was not affected (Fig. 4E). Since we used pCox4 in our SPR analysis, we also imported the Cox4 precursor into WT, *tom70*Δ/ *tom71*Δ and $tom70^{M551R}$ mitochondria (Fig. 4F). The import of the matrix protein Cox4 showed no defect in these strains, similar to Su9-DHFR.

Carrier substrates are characterized by the presence of multiple transmembrane segments and depend on cytosolic chaperones for their import. We therefore reasoned that even though Tom70 does not influence the import of model matrix proteins (such as Su9-DHFR or Cox4) [54], it could affect the import of presequence-containing substrates which contain multiple transmembrane segments. The ABC transporter Mdl1 is a presequence-containing protein with six transmembrane segments and was previously shown to be imported by TIM23 and inserted into the inner membrane by TIM23 and OXA1 [13,14,17,55]. Confirming our assumption, the import of radiolabeled Mdl1 was strongly reduced in *tom70*Δ/ *tom71*Δ mitochondria (Fig. 4G).

In order to delineate a possible Tom70 chaperoning effect [54], from bona fide presequence binding, we tested import into the $tom70^{M551R}$ mutant, which showed no AAC import defect but a decrease in presequence binding *in vitro* (Fig. 4D and 3G). Interestingly, the Mdl1 import efficiency was only ~50% in the $tom70^{M551R}$ mutant mitochondria (Fig. 4G and H).

Collectively, these results demonstrate that a single point mutation in the binding cleft in Tom70 decreases the presequence binding *in vitro* and selectively reduces import of the presequence-containing membrane protein Mdl1.

In line with previous reports, presequence recognition by Tom70 is not essential for general presequence import, as matrix targeted precursors are not affected by the M551R mutation or the deletion of *TOM70*. However, import of an inner membrane protein, as exemplified by Mdl1 that contains several transmembrane segments, is facilitated by presequence recognition by Tom70. Several arguments support this: I) Tom70 binds directly to presequence peptides with its binding groove, in this case irrespective of a mature segment. II) Mdl1 import depends on Tom70. III) The M551R mutation does not affect carrier import but selectively reduces Mdl1 import efficiency and presequence recognition *in vitro*. We conclude that Tom70 can recognize presequences of a limited set of presequence-containing precursors, as exemplified by Mdl1, and thereby stimulates their mitochondrial import.

4. Conclusion

Our study reveals that the cytosolic domain of Tom70 is capable of binding presequence peptides, both *in vitro* and *in organello*. This direct interaction is mediated through the binding groove constituted by the C-terminal domain containing TPR 4–11 and requires a semi-open or open conformation. Transition between the closed and open state involves movement of the N-terminal domain away from the C-terminal domain. During this conformational change, the helix A7 swings away from the binding cleft (Fig. 5). In the semi-open conformation the cleft is wide enough to accommodate a helical ligand, which based on our docking analysis partially overlaps with the position of helix A7 in the closed state. It will be interesting to investigate the physiological relevance of a possible auto-inhibition mechanism by helix A7 and the impact of Hsp70 binding on the conformational state of Tom70.

A single point mutation (M551R), which introduces an extra positive charge in the binding groove, decreased presequence binding affinity ten-fold. The mutant protein supports wild-type import of carrier proteins, but revealed a specific requirement of presequence recognition for the import of the inner membrane protein Mdl1. Hence the recognition of carrier substrates and contribution to presequence import are distinct features of the Tom70 structure.

Acknowledgement

We are grateful to O. Bernhard and K. Neifer for their excellent technical assistance and to Dr. M. van der Laan for providing the Mdl1 plasmid. The study was supported by the Deutsche Forschungsgemeinschaft,

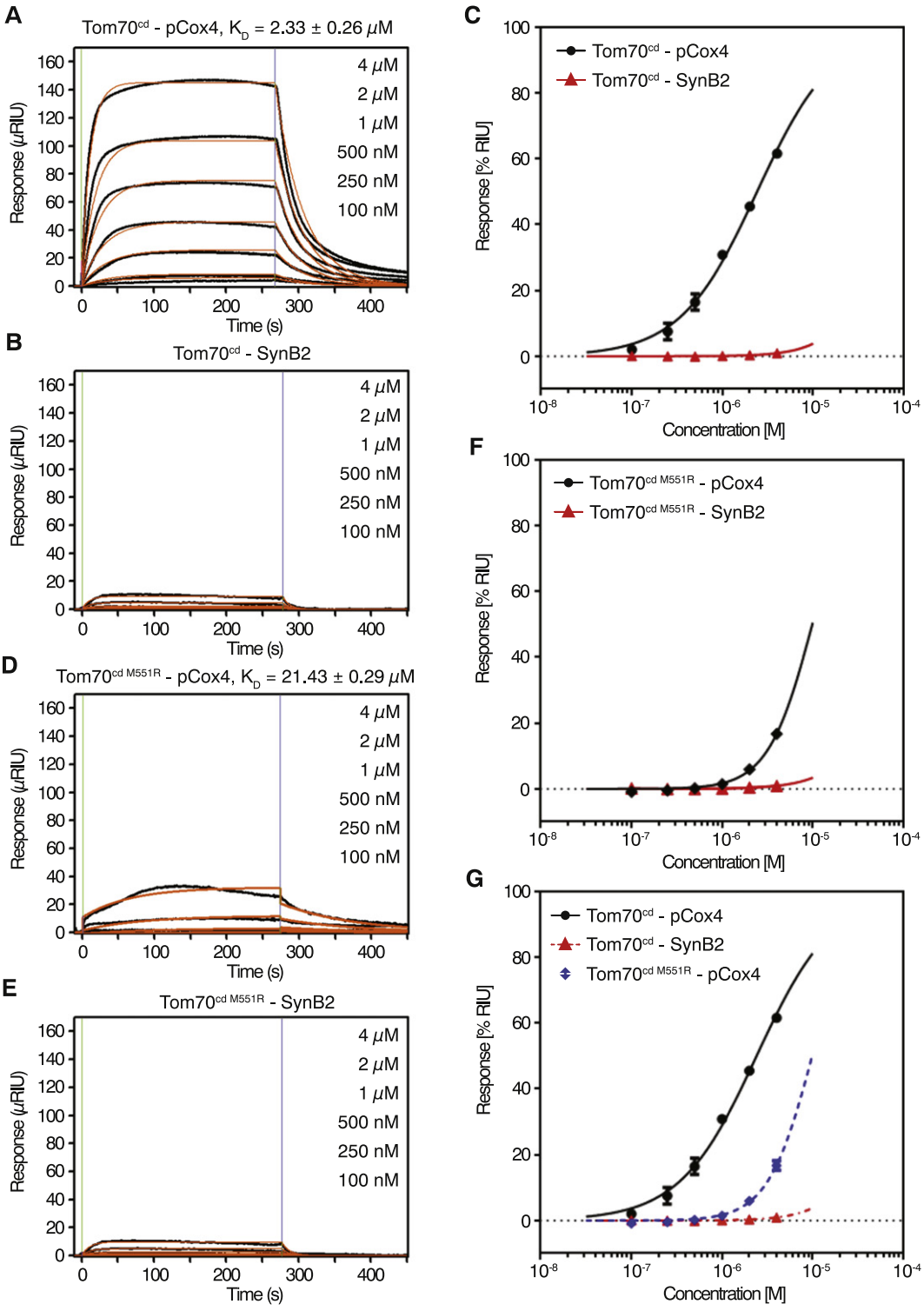

Fig. 3. Characterization of the Tom70-presequence interaction. *A)* Purified, His-tagged, cytosolic domain of wild-type Tom70 was immobilized on a chip and the SPR response was recorded after injection of the indicated concentrations of Cox4 presequence peptide (pCox4). A typical sensogram is shown. Recorded response, black lines; kinetic fit k_a and k_d, orange lines. K_D is indicated as mean ± SEM ($n \geq 3$). *B)* SPR response recorded for binding of the control peptide SynB2 to Tom70^{cd}. Experiment performed as in A. No binding was observed; accordingly no affinity constant was determined. *C)* Equilibrium binding isotherms of maximal response vs. analyte concentration are shown for wild-type Tom70^{cd} and pCox4 or SynB2 (data fitting for a one to one interaction). *D)* Interactions of M551R Tom70^{cd} with pCox4 was recorded and a kinetic fit was devised as for A. *E)* SPR response recorded for binding of the control peptide SynB2 to M551R Tom70^{cd}. Processed as in A. *F)* Equilibrium binding isotherms of M551R Tom70^{cd} and pCox4 or SynB2. *G)* Comparison of the equilibrium binding isotherms of binding of pCox4 or SynB2 to wild-type or M551R Tom70^{cd}.

SFB860, FOR 1086/2 (Grant SCHW 823/2-1) (MK, SPR Biosensor SR7000DC), the PhD program 'Molecular Biology' — International Max Planck Research School and the Göttingen Graduate School for Neurosciences and Molecular Biosciences (GGNB) (DFG grant GSC 226/1) at the Georg August University Göttingen (JM, RG and AS), Boehringer Ingelheim Fonds (CS) and the Max Planck Society (PR).

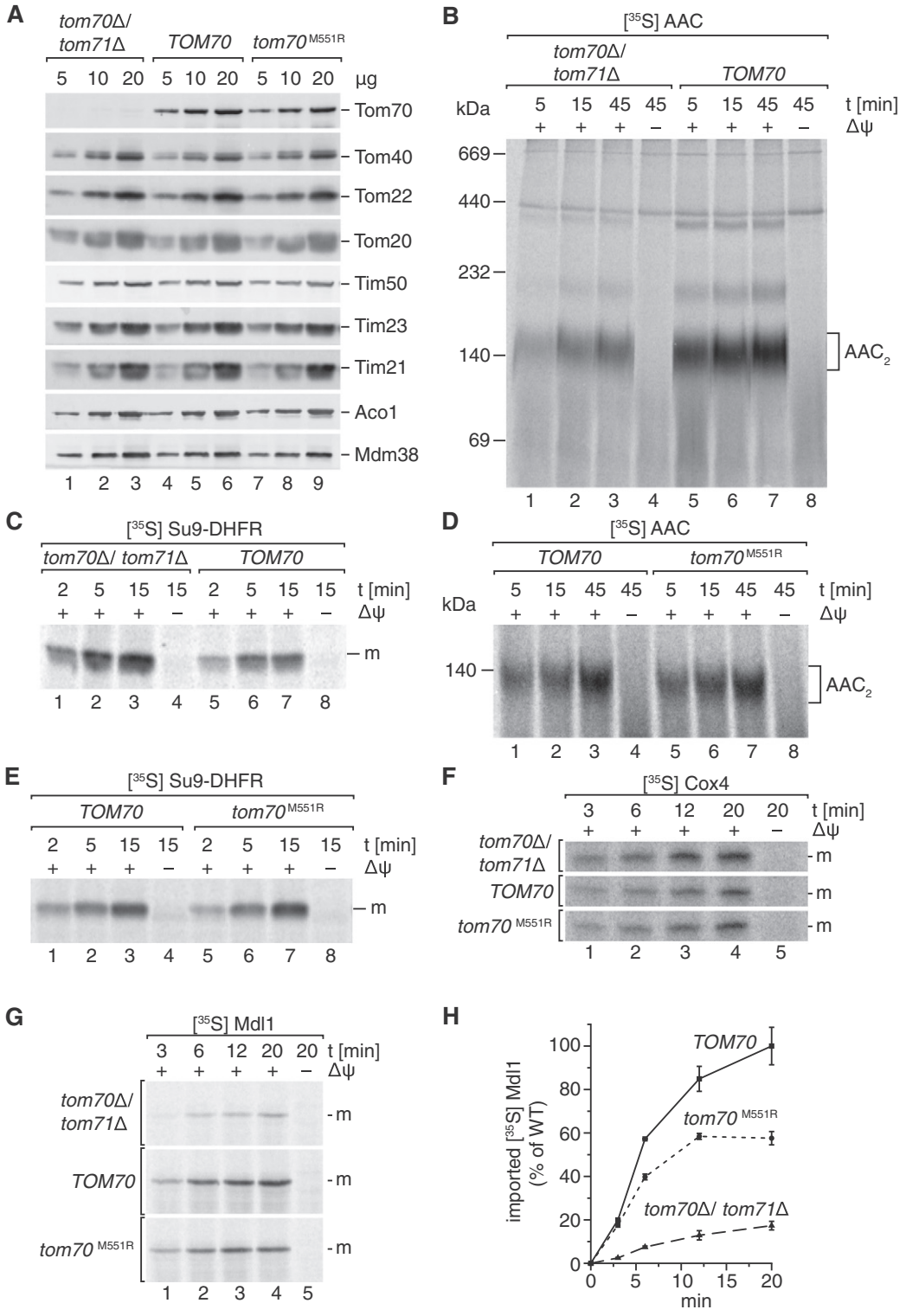

Fig. 4. Mutation of Tom70's presequence binding site specifically affects Mdl1 import. *A)* Steady state analysis of isolated *tom70Δ/ tom71Δ*, wild-type (*TOM70*) and *tom70*^{M551R} mitochondria. Indicated amounts were analyzed by SDS–PAGE and Western blotting. *B)* Import and assembly of radiolabeled AAC in isolated *tom70Δ/ tom71Δ* and wild-type (*TOM70*) mitochondria for the indicated times. The reactions were stopped by dissipation of the membrane potential (Δψ) and proteinase K treatment. Samples were analyzed by BN–PAGE and autoradiography. AAC_2 – assembled dimer of AAC. *C)* Import of radiolabeled Su9-DHFR into isolated *tom70Δ/ tom71Δ* and wild-type (*TOM70*) mitochondria for the indicated times. The reactions were stopped by dissipation of the membrane potential (Δψ) and proteinase K treatment. Samples were analyzed by SDS–PAGE and autoradiography. m, mature protein. *D)* Import and assembly of radiolabeled AAC into isolated wild-type (*TOM70*) and *tom70*^{M551R} mitochondria as described in B. AAC_2 – assembled dimer of AAC. *E)* Import of radiolabeled Su9-DHFR into isolated wild-type (*TOM70*) and *tom70*^{M551R} mitochondria as described in C. *F)* Import of radiolabeled Cox4 into isolated *tom70Δ/ tom71Δ*, wild-type (*TOM70*) and *tom70*^{M551R} mitochondria for the indicated times. The reactions were stopped by dissipation of the membrane potential (Δψ) and proteinase K treatment. Samples were analyzed as in C. m, mature protein. *G)* Import of radiolabeled Mdl1 into *tom70Δ/ tom71Δ*, wild-type (*TOM70*) and *tom70*^{M551R} mitochondria as described in F. m, mature protein. *H)* Quantification of the Mdl1 import efficiency as performed in G. Import efficiency after 20 min in the wild-type was set to 100% (mean ± SEM, n = 3).

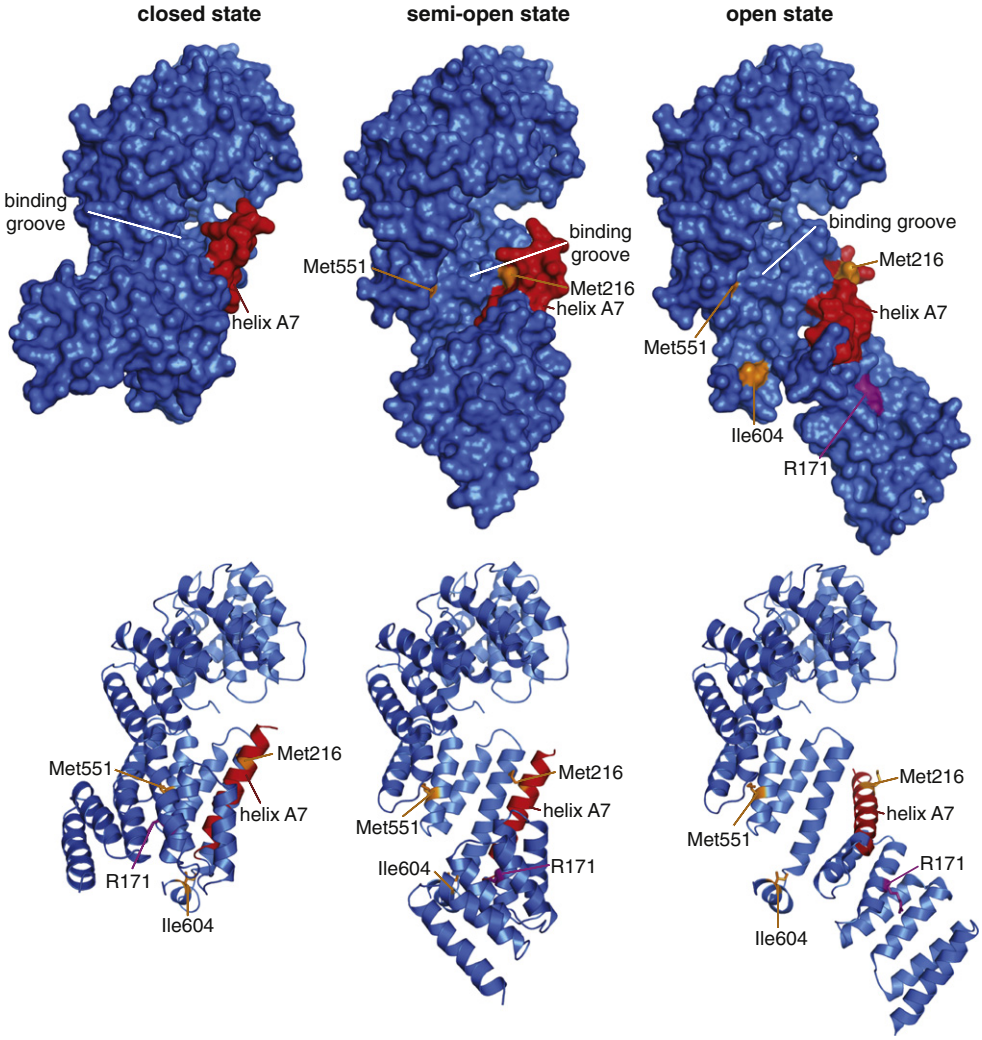

Fig. 5. Differences between the closed (left, 2GW1), semi-open (middle, homology model based on the open Tom71 structure, 3LCA, and relative movement of the N-terminal to the C-terminal domain) and open (right, homology model based on the open Tom71 structure, 3LCA) state of Tom70 shown with surface (top) or cartoon representation (bottom). Residues identified to be cross-linked to $pL_{19}B$ are colored in orange, Arg171 (purple) represents the Hsp70 binding site. The transition from the closed to the open sate involves displacement of helix A7 (red). While it partially occupies the binding groove in the closed state, it contributes to the wall of the groove in the semi-open and open state.

References

[1] A. Chacinska, C.M. Koehler, D. Milenkovic, T. Lithgow, N. Pfanner, Importing mitochondrial proteins: machineries and mechanisms, Cell 138 (2009) 628–644, http://dx.doi.org/10.1016/j.cell.2009.08.005.

[2] T. Becker, L. Böttinger, N. Pfanner, Mitochondrial protein import: from transport pathways to an integrated network, Trends Biochem. Sci. (2011) 1–7, http://dx.doi.org/10.1016/j.tibs.2011.11.004.

[3] J. Dudek, P. Rehling, M. van der Laan, Mitochondrial protein import: common principles and physiological networks, Biochim. Biophys. Acta 1833 (2013) 274–285, http://dx.doi.org/10.1016/j.bbamcr.2012.05.028.

[4] C. Schulz, A. Schendzielorz, P. Rehling, Unlocking the presequence import pathway, Trends Cell Biol. 25 (2015) 265–275, http://dx.doi.org/10.1016/j.tcb.2014.12.001.

[5] K. Verner, Co-translational protein import into mitochondria: an alternative view, Trends Biochem. Sci. 18 (1993) 366–371.

[6] E. Eliyahu, L. Pnueli, D. Melamed, T. Scherrer, A.P. Gerber, O. Pines, et al., Tom20 mediates localization of mRNAs to mitochondria in a translation-dependent manner, Mol. Cell. Biol. 30 (2009) 284–294, http://dx.doi.org/10.1128/MCB.00651-09.

[7] M. Opalińska, C. Meisinger, Metabolic control via the mitochondrial protein import machinery, Curr. Opin. Cell Biol. 33C (2014) 42–48, http://dx.doi.org/10.1016/j.ceb.2014.11.001.

[8] K. Dietmeier, A. Hönlinger, U. Bömer, P.J. Dekker, C. Eckerskorn, F. Lottspeich, et al., Tom5 functionally links mitochondrial preprotein receptors to the general import pore, Nature 388 (1997) 195–200, http://dx.doi.org/10.1038/40663.

[9] Y. Abe, T. Shodai, T. Muto, K. Mihara, H. Torii, S. Nishikawa, et al., Structural basis of presequence recognition by the mitochondrial protein import receptor Tom20, Cell 100 (2000) 551–560.

[10] D. Rapaport, W. Neupert, R. Lill, Mitochondrial protein import. Tom40 plays a major role in targeting and translocation of preproteins by forming a specific binding site for the presequence, J. Biol. Chem. 272 (1997) 18725–18731.

[11] J. Melin, C. Schulz, L. Wrobel, O. Bernhard, A. Chacinska, O. Jahn, et al., Presequence recognition by the Tom40 channel contributes to precursor translocation into the mitochondrial matrix, Mol. Cell. Biol. 34 (2014) 3473–3485, http://dx.doi.org/10.1128/MCB.00433-14.

[12] K. Hell, J.M. Herrmann, E. Pratje, W. Neupert, R.A. Stuart, Oxa1p, an essential component of the N-tail protein export machinery in mitochondria, Proc. Natl. Acad. Sci. U. S. A. 95 (1998) 2250–2255.

[13] M. Bohnert, P. Rehling, B. Guiard, J.M. Herrmann, N. Pfanner, M. van der Laan, Cooperation of stop-transfer and conservative sorting mechanisms in mitochondrial protein transport, Curr. Biol. 20 (2010) 1227–1232, http://dx.doi.org/10.1016/j.cub.2010.05.058.

[14] L. Young, K. Leonhard, T. Tatsuta, J. Trowsdale, T. Langer, Role of the ABC transporter Mdl1 in peptide export from mitochondria, Science 291 (2001) 2135–2138, http://dx.doi.org/10.1126/science.1056957.

[15] M. Hofacker, S. Gompf, A. Zutz, C. Presenti, W. Haase, C. van der Does, et al., Structural and functional fingerprint of the mitochondrial ATP-binding cassette transporter Mdl1 from *Saccharomyces cerevisiae*, J. Biol. Chem. 282 (2007) 3951–3961, http://dx.doi.org/10.1074/jbc.M609899200.

[16] K. Park, S.C. Botelho, J. Hong, M. Osterberg, H. Kim, Dissecting stop transfer versus conservative sorting pathways for mitochondrial inner membrane proteins *in vivo*, J. Biol. Chem. 288 (2013) 1521–1532, http://dx.doi.org/10.1074/jbc.M112.409748.

[17] K. Park, S. Jung, H. Kim, H. Kim, Mode of membrane insertion of individual transmembrane segments in Mdl1 and Mdl2, multi-spanning mitochondrial ABC transporters, FEBS Lett. (2014) 1–9, http://dx.doi.org/10.1016/j.febslet.2014.08.001.

[18] N. Wiedemann, N. Pfanner, M.T. Ryan, The three modules of ADP/ATP carrier cooperate in receptor recruitment and translocation into mitochondria, EMBO J. 20 (2001) 951–960, http://dx.doi.org/10.1093/emboj/20.5.951.
[19] J.C. Young, N.J. Hoogenraad, F.U. Hartl, Molecular chaperones Hsp90 and Hsp70 deliver preproteins to the mitochondrial import receptor Tom70, Cell 112 (2003) 41–50.
[20] Y. Wu, B. Sha, Crystal structure of yeast mitochondrial outer membrane translocon member Tom70p, Nat. Struct. Mol. Biol. 13 (2006) 589–593, http://dx.doi.org/10.1038/nsmb1106.
[21] P. Rehling, K. Model, K. Brandner, P. Kovermann, A. Sickmann, H.E. Meyer, et al., Protein insertion into the mitochondrial inner membrane by a twin-pore translocase, Science 299 (2003) 1747–1751, http://dx.doi.org/10.1126/science.1080945.
[22] V. Hines, A. Brandt, G. Griffiths, H. Horstmann, H. Brütsch, G. Schatz, Protein import into yeast mitochondria is accelerated by the outer membrane protein MAS70, EMBO J. 9 (1990) 3191–3200.
[23] V. Hines, G. Schatz, Precursor binding to yeast mitochondria. A general role for the outer membrane protein Mas70p, J. Biol. Chem. 268 (1993) 449–454.
[24] N. Hachiya, K. Mihara, K. Suda, M. Horst, G. Schatz, T. Lithgow, Reconstitution of the initial steps of mitochondrial protein import, Nature 376 (1995) 705–709, http://dx.doi.org/10.1038/376705a0.
[25] M. Kurz, H. Martin, J. Rassow, N. Pfanner, M.T. Ryan, Biogenesis of Tim proteins of the mitochondrial carrier import pathway: differential targeting mechanisms and crossing over with the main import pathway, Mol. Biol. Cell 10 (1999) 2461–2474.
[26] J. Brix, K. Dietmeier, N. Pfanner, Differential recognition of preproteins by the purified cytosolic domains of the mitochondrial import receptors Tom20, Tom22, and Tom70, J. Biol. Chem. 272 (1997) 20730–20735.
[27] T. Komiya, S. Rospert, G. Schatz, K. Mihara, Binding of mitochondrial precursor proteins to the cytoplasmic domains of the import receptors Tom70 and Tom20 is determined by cytoplasmic chaperones, EMBO J. 16 (1997) 4267–4275.
[28] J. Brix, S. Rüdiger, B. Bukau, J. Schneider-Mergener, N. Pfanner, Distribution of binding sequences for the mitochondrial import receptors Tom20, Tom22, and Tom70 in a presequence-carrying preprotein and a non-cleavable preprotein, J. Biol. Chem. 274 (1999) 16522–16530.
[29] J. Li, X. Qian, J. Hu, B. Sha, Molecular chaperone Hsp70/Hsp90 prepares the mitochondrial outer membrane translocon receptor Tom71 for preprotein loading, J. Biol. Chem. 284 (2009) 23852–23859, http://dx.doi.org/10.1074/jbc.M109.023986.
[30] J. Li, W. Cui, B. Sha, The structural plasticity of Tom71 for mitochondrial precursor translocations, Acta Crystallogr. Sect. F: Struct. Biol. Cryst. Commun. 66 (2010) 985–989, http://dx.doi.org/10.1107/S1744309110025522.
[31] M. Moczko, B. Ehmann, F. Gärtner, A. Hönlinger, E. Schäfer, N. Pfanner, Deletion of the receptor MOM19 strongly impairs import of cleavable preproteins into *Saccharomyces cerevisiae* mitochondria, J. Biol. Chem. 269 (1994) 9045–9051.
[32] D. Stojanovski, N. Pfanner, N. Wiedemann, Import of proteins into mitochondria, Methods Cell Biol. 80 (2007) 783–806, http://dx.doi.org/10.1016/S0091-679X(06)80036-1.
[33] C. Schulz, O. Lytovchenko, J. Melin, A. Chacinska, B. Guiard, P. Neumann, et al., Tim50's presequence receptor domain is essential for signal driven transport across the TIM23 complex, J. Cell Biol. 195 (2011) 643–656, http://dx.doi.org/10.1083/jcb.201105098.
[34] O. Jahn, K. Eckart, O. Brauns, H. Tezval, J. Spiess, The binding protein of corticotropin-releasing factor: ligand-binding site and subunit structure, Proc. Natl. Acad. Sci. U. S. A. 99 (2002) 12055–12060, http://dx.doi.org/10.1073/pnas.192449299.
[35] M. Götze, J. Pettelkau, S. Schaks, K. Bosse, C.H. Ihling, F. Krauth, et al., StavroX–a software for analyzing crosslinked products in protein interaction studies, J. Am. Soc. Mass Spectrom. 23 (2012) 76–87, http://dx.doi.org/10.1007/s13361-011-0261-2.
[36] B. Raveh, N. London, L. Zimmerman, O. Schueler-Furman, Rosetta FlexPepDock ab-initio: simultaneous folding, docking and refinement of peptides onto their receptors, PLoS ONE 6 (2011) e18934, http://dx.doi.org/10.1371/journal.pone.0018934.
[37] G.M. Morris, R. Huey, W. Lindstrom, M.F. Sanner, R.K. Belew, D.S. Goodsell, et al., AutoDock4 and AutoDockTools4: automated docking with selective receptor flexibility, J. Comput. Chem. 30 (2009) 2785–2791, http://dx.doi.org/10.1002/jcc.21256.
[38] O. Trott, A.J. Olson, AutoDock Vina: improving the speed and accuracy of docking with a new scoring function, efficient optimization, and multithreading, J. Comput. Chem. 31 (2) (2009) 455–461.
Wiley Online Library, J. Comput. Chem. (2010).
[39] I. Forné, J. Ludwigsen, A. Imhof, P.B. Becker, F. Mueller-Planitz, Probing the conformation of the ISWI ATPase domain with genetically encoded photoreactive crosslinkers and mass spectrometry, Mol. Cell. Proteomics 11 (2012)http://dx.doi.org/10.1074/mcp.M111.012088 (M111.012088).
[40] O. Lytovchenko, J. Melin, C. Schulz, M. Kilisch, D.P. Hutu, P. Rehling, Signal recognition initiates reorganization of the presequence translocase during protein import, EMBO J. 32 (2013) 886–898, http://dx.doi.org/10.1038/emboj.2013.23.
[41] C. Schulz, P. Rehling, Remodelling of the active presequence translocase drives motor-dependent mitochondrial protein translocation, Nat. Commun. 5 (2014) 4349, http://dx.doi.org/10.1038/ncomms5349.
[42] V. Neuhoff, N. Arold, D. Taube, W. Ehrhardt, Improved staining of proteins in polyacrylamide gels including isoelectric focusing gels with clear background at nanogram sensitivity using Coomassie Brilliant Blue G-250 and R-250, Electrophoresis 9 (1988) 255–262, http://dx.doi.org/10.1002/elps.1150090603.
[43] T. Beddoe, S.R. Bushell, M.A. Perugini, T. Lithgow, T.D. Mulhern, S.P. Bottomley, et al., A biophysical analysis of the tetratricopeptide repeat-rich mitochondrial import receptor, Tom70, reveals an elongated monomer that is inherently flexible, unstable, and unfolds via a multistate pathway, J. Biol. Chem. 279 (2004) 46448–46454, http://dx.doi.org/10.1074/jbc.M405639200.
[44] R. Mills, J. Trewhella, T. Qiu, T. Welte, T. Ryan, T. Hanley, et al., Domain organization of the monomeric form of the Tom70 mitochondrial import receptor, J. Mol. Biol. 388 (2009) 1043–1058, http://dx.doi.org/10.1016/j.jmb.2009.03.070.
[45] T. Endo, D. Kohda, Functions of outer membrane receptors in mitochondrial protein import, Biochim. Biophys. Acta 1592 (2002) 3–14.
[46] T. Söllner, R. Pfaller, G. Griffiths, N. Pfanner, W. Neupert, A mitochondrial import receptor for the ADP/ATP carrier, Cell 62 (1990) 107–115.
[47] H.F. Steger, T. Söllner, M. Kiebler, K.A. Dietmeier, R. Pfaller, K.S. Trülzsch, et al., Import of ADP/ATP carrier into mitochondria: two receptors act in parallel, J. Cell Biol. 111 (1990) 2353–2363.
[48] J. Schlossmann, R. Lill, W. Neupert, D.A. Court, Tom71, a novel homologue of the mitochondrial preprotein receptor Tom70, J. Biol. Chem. 271 (1996) 17890–17895.
[49] M.T. Ryan, H. Müller, N. Pfanner, Functional staging of ADP/ATP carrier translocation across the outer mitochondrial membrane, J. Biol. Chem. 274 (1999) 20619–20627.
[50] A. Geissler, A. Chacinska, K. Truscott, N. Wiedemann, K. Brandner, A. Sickmann, et al., The mitochondrial presequence translocase: an essential role of Tim50 in directing preproteins to the import channel, Cell 111 (2002) 507–518.
[51] H. Yamamoto, M. Esaki, T. Kanamori, Y. Tamura, S. ichi Nishikawa, T. Endo, Tim50 is a subunit of the TIM23 complex that links protein translocation across the outer and inner mitochondrial membranes, Cell 111 (2002) 519–528.
[52] A.E. Frazier, J. Dudek, B. Guiard, W. Voos, Y. Li, M. Lind, et al., Pam16 has an essential role in the mitochondrial protein import motor, Nat. Struct. Mol. Biol. 11 (2004) 226–233, http://dx.doi.org/10.1038/nsmb735.
[53] A. Chacinska, M. Lind, A.E. Frazier, J. Dudek, C. Meisinger, A. Geissler, et al., Mitochondrial presequence translocase: switching between TOM tethering and motor recruitment involves Tim21 and Tim17, Cell 120 (2005) 817–829, http://dx.doi.org/10.1016/j.cell.2005.01.011.
[54] H. Yamamoto, K. Fukui, H. Takahashi, S. Kitamura, T. Shiota, K. Terao, et al., Roles of Tom70 in import of presequence-containing mitochondrial proteins, J. Biol. Chem. 284 (2009) 31635–31646, http://dx.doi.org/10.1074/jbc.M109.041756.
[55] A. Zutz, S. Gompf, H. Schägger, R. Tampé, Mitochondrial ABC proteins in health and disease, Biochim. Biophys. Acta 1787 (2009) 681–690, http://dx.doi.org/10.1016/j.bbabio.2009.02.009.
[56] J. Pettelkau, C.H. Ihling, P. Frohberg, L. van Werven, O. Jahn, A. Sinz, Reliable identification of cross-linked products in protein interaction studies by 13c-labeled p-benzoylphenylalanine, J. Am. Soc. Mass Spectrom. 25 (2014) 1628–1641, http://dx.doi.org/10.1007/s13361-014-0944-6.